ARTICLE

Check for updates

Mantle plume and rift-related volcanism during the evolution of the Rio Grande Rise

Patrick A. Hoyer [1✉], Karsten M. Haase[1], Marcel Regelous[1], John M. O'Connor[1,2], Stephan Homrighausen[3], Wolfram H. Geissler [4] & Wilfried Jokat [4,5]

The Rio Grande Rise in the western South Atlantic Ocean has been interpreted as either an oceanic plateau related to the Tristan-Gough mantle plume, or a fragment of detached continental crust. Here we present new major and trace element data for volcanic rocks from the western and eastern Rio Grande Rise and the adjacent Jean Charcot Seamount Chain. The eastern Rio Grande Rise and older parts of the western Rio Grande Rise are comprised of tholeiitic basalt with moderately enriched trace element compositions and likely formed above the Tristan-Gough mantle plume close to the southern Mid-Atlantic Ridge. Younger alkalic lavas from the western Rio Grande Rise and the Jean Charcot Seamount Chain were formed by lower degrees of melting beneath thicker lithosphere in an intraplate setting possibly during rifting of the plateau. There is no clear geochemical evidence that remnants of continental crust are present beneath the Rio Grande Rise.

[1] Friedrich-Alexander-Universität Erlangen-Nürnberg (FAU), GeoZentrum Nordbayern, Erlangen, Germany. [2] Vrije Universiteit Amsterdam, Amsterdam, The Netherlands. [3] Geomar—Helmholtz-Zentrum für Ozeanforschung Kiel, Kiel, Germany. [4] Alfred Wegener Institut—Helmholtz-Zentrum für Polar- und Meeresforschung, Bremerhaven, Germany. [5] University of Bremen, Department of Geoscience, Bremen, Germany. ✉email: patrick.hoyer@fau.de

large regions of the ocean basins are covered by bathymetric swells that formed by excess magmatism either in deep mantle plumes or at subduction zones, and by rifting of continental fragments. Oceanic plateaus, volcanic ridges and age-progressive volcanic seamount chains are usually attributed to anomalously hot mantle material rising in a plume from the deep mantle resulting in partial melting and formation of crust up to 35 km thick[1,2]. Some of the largest plateaus may have formed above mantle plumes close to spreading ridges, where decompression melting is enhanced. However, some oceanic plateaus represent slivers of ancient continental crust related to continental rifting (e.g. the Seychelles and Jan Mayen microcontinents[3,4]), some of which are covered by young basaltic lavas (e.g. Mauritius and Mascarene Plateau[5]).

The Rio Grande Rise (RGR) and the Walvis Ridge (Fig. 1) are the most prominent bathymetric features of the South Atlantic Ocean and have been interpreted as a Large Igneous Province of volcanic origin related to the Tristan-Gough mantle plume[6–8]. Between ~120 and ~80 Ma, this plume was situated beneath or in close proximity to the Mid-Atlantic Ridge resulting in the formation of the Walvis Ridge and western RGR (WRGR) on the African and South American Plates respectively, in a setting that was similar to present-day Iceland[9–11]. Trace element and Sr-Nd-Hf-Pb isotopic data, as well as ^{40}Ar–^{39}Ar ages (80–87 Ma) of tholeiitic lavas from Deep Sea Drilling Project (DSDP) Site 516[12–14] on the WRGR (Fig. 1), are in accordance with a joint formation with the Walvis Ridge at the Mid-Atlantic Ridge[15,16]. Between 80 and 60 Ma, continuous volcanic activity separated the Walvis Ridge and WRGR along a southward propagating plume-fed spreading axis, which subsequently led to the formation of the N-S trending eastern RGR (ERGR) and its corresponding counterpart on the African Plate[9,10]. Compared to the WRGR, much less is known about the origin and evolution of the ERGR, and it has not been previously sampled. At ~60 Ma, the Walvis Ridge and RGR were finally separated by several ridge jumps, which isolated the RGR on the South American Plate and temporarily terminated its magmatic formation[17]. Plume-related volcanism continued on the African Plate forming the Guyot Province consisting of two age-progressive and isotopically distinct volcanic tracks extending from the Walvis Ridge to the volcanically-active ocean islands of Tristan da Cunha and Gough[16]. Recent ^{40}Ar–^{39}Ar ages from the samples recovered from the crest of WRGR indicate a later volcanic event at ~46 Ma[16,18,19] with a distinct geochemical signature compared to the main plateau forming stage[20]. At about this time, the RGR was cut by the NW-SE trending Cruzeiro do Sul Rift (CdSR) that is up to 20 km wide and 1 km deep[21] (Fig. 1). Since the CdSR also affected the Brazilian continental margin forming the Cabo Frio High[22], it is believed to reflect a major plate reorganization in the Paleogene and Neogene[21]. A recent re-examination of a multichannel seismic reflection profile suggests that the formation of the CdSR could have started earlier during the Late Cretaceous[23]. Satellite altimetry maps reveal a chain of seamounts in the northwestern prolongation of the CdSR extending towards the Cabo Frio High[24] (Fig. 1). This so-called Jean Charcot Seamount Chain (JCSC) has not been previously sampled, so its age and relationship to the formation of WRGR and CdSR are unknown.

In contrast to exclusively magmatic models, recent geophysical and petrological studies claim that the WRGR is a continental crustal fragment detached from the Brazilian margin that has been preserved as a 'microcontinent' embedded in plume-influenced oceanic crust[25,26]. The submarine plateau exhibits a negative Bouguer anomaly indicating a mass deficiency relative to the surrounding seafloor[21]. Further, submersible sampling recovered boulders of gneiss, granite and pegmatite of Proterozoic age suggesting that the WRGR may be underlain by slivers of

continental crust[25]. These recent findings seem to contradict the previous models for the volcanic origin of the RGR[25,26].

Here we present major and trace element data for new samples of volcanic rocks recently dredged from the eastern and western RGR as well as the adjacent JCSC. We use petrological and geochemical data to examine the petrogenesis and tectonic setting of formation of these oceanic volcanic structures, their relationship to the Tristan-Gough mantle plume, the Walvis Ridge and the CdSR, and investigate whether there is evidence for the presence of remnants of continental crust in the area of the RGR. To address these questions, we also present major and trace element compositions for volcanic rocks drilled from DSDP Site 516 which serve as a reference for the local geochemical signature. Our geochemical study contributes to the understanding of the volcanic processes on the South American Plate during the opening of the South Atlantic Ocean.

Results

Petrography and mineralogy. The ERGR samples were dredged from the northern shoulder of the CdSR from depths between 915 and 5266 m below sea level (Fig. 1b). The common rocks in this area are fine- to medium-grained aphanitic basalts with weak to moderate seawater alteration and manganese oxide/hydroxide crusts up to 4 cm on surfaces. Furthermore, porphyritic basalts with phenocrysts of plagioclase and/or clinopyroxene embedded in a fine-grained matrix occur. Both aphanitic and porphyritic rocks contain numerous vesicles of variable size and shape, which are filled with calcite and/or brownish alteration material. Rarely, volcanic breccias composed of angular to rounded basaltic fragments were sampled.

The samples from the WRGR were dredged from both the southern and northern flanks of the CdSR in water depths between 1100 and 4500 m below sea level (Fig. 1b). In contrast to the lavas from the ERGR, those from the WRGR are more heterogeneous ranging from mafic to intermediate compositions. Both aphanitic and porphyritic textures are common, whereby phenocrysts of plagioclase and/or clinopyroxene are the dominant mineral phases within the latter. Most rocks have thin manganese oxide/hydroxide coatings on their surfaces, while only a few show distinctive crusts with up to 3 cm thickness. In general, the samples are less affected by seawater alteration, but strong seawater alteration occurs along cracks. The majority of rocks contain vesicles that are filled with calcite and/or brownish material. Volcanic breccias composed of mafic to intermediate rock fragments are more common compared to the ERGR.

The DSDP Site 516 samples were obtained from two sections of Core 128 of DSDP Hole 516 F[27] (Fig. 1b). One sample each was taken from the intervals 23–24, 58–59 and 124–125 of core 128-1 as well as from the intervals 26–27 and 37–38 of core 128-2. The samples display a glomerophyric texture with phenocrysts of plagioclase and clinopyroxene occurring as small clusters embedded within a fine-grained matrix[14]. Vesicles are rare and filled with greenish clay minerals, chlorite and calcite[14].

The samples from the JCSC were dredged from steep slopes of distinct submarine volcanoes from depths between 1780 and 3335 m below sea level (Fig. 1b). The rocks display both aphanitic and porphyritic textures with phenocrysts of plagioclase, clinopyroxene and/or altered olivine. The matrix is predominantly fine-grained with common sub-rounded to rounded vesicles. The majority of rocks show weak alteration along with fractures, but exhibit MnOOH coatings or crusts (up to 2 cm) on their surfaces.

Geochemistry. In total, 27 samples from the ERGR (from seven sites), 20 samples from the WRGR (from six sites), 31 samples
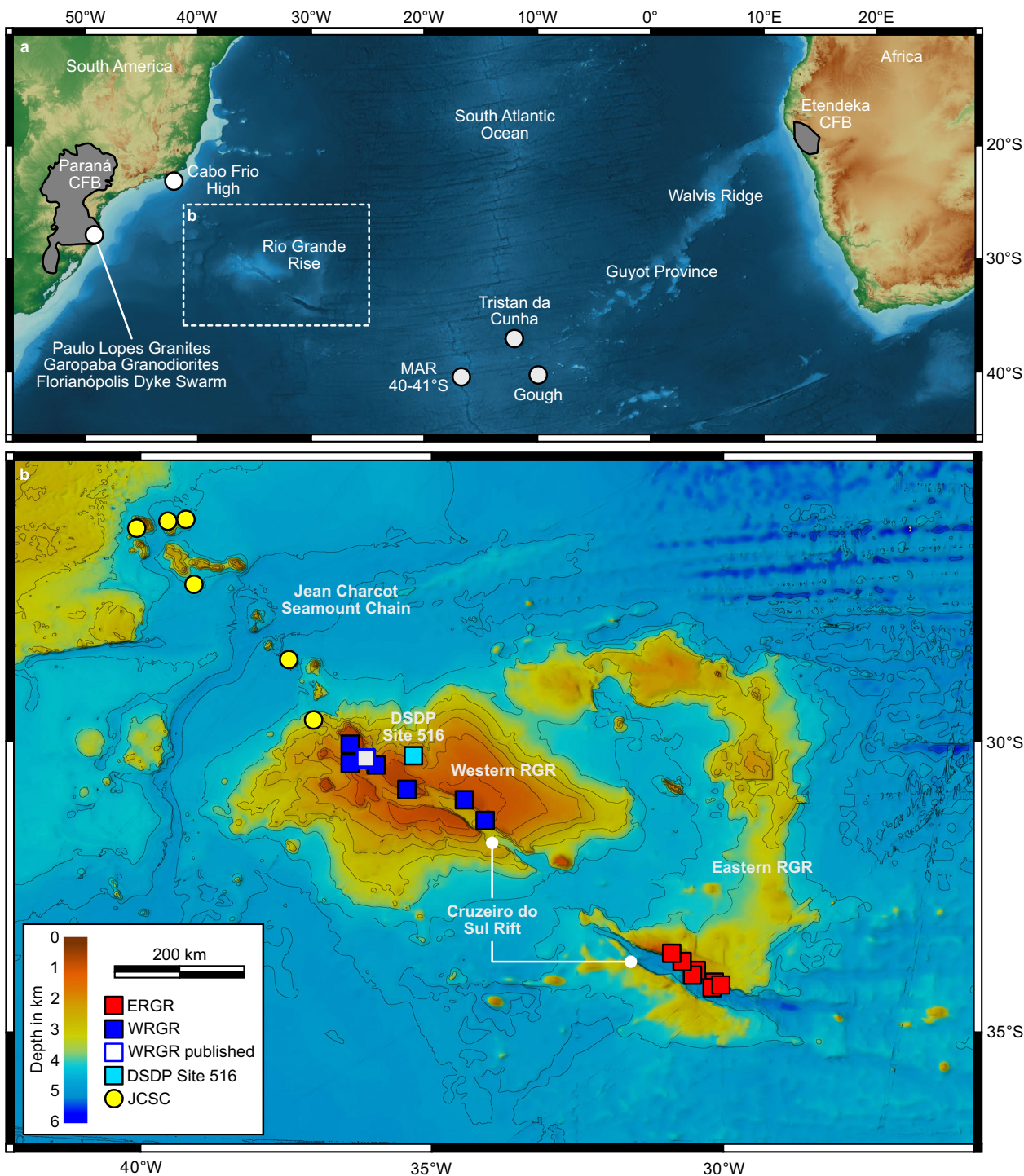
Fig. 1 Bathymetric map of the South Atlantic Ocean. a The map shows the locations of the Rio Grande Rise and Walvis Ridge. Grey areas on the South American and African continents are the Paraná and Etendeka Continental flood basalt provinces (CFBs), respectively. MAR stands for Mid-Atlantic Ridge. **b** Zoomed map section from **a**. Detailed map of the Rio Grande Rise showing the Eastern Rio Grande Rise (ERGR), Western Rio Grande Rise (WRGR) and the Jean Charcot Seamount Chain (JCSC). The blue framed white square marks the position of a dredge site from where alkaline samples with an age of ~46 Ma[16,18] were previously collected. White arrows mark the deep valley of the Cruzeiro do Sul Rift (CdSR). Contour line interval is 500 m. Digital elevation models are based on the GEBCO_2020 Grid (http://www.gebco.net).

from the JCSC (from six sites) and five samples from DSDP Site 516 (Fig. 1) were analyzed for their major and trace element compositions and the results are provided in Supplementary Data 1. Although our samples were carefully selected and only the freshest parts of each rock were used for geochemical analysis, the loss on ignition ranges from 0.7 to 26 wt.%. To minimize the

effects of secondary alteration processes on the major and trace element concentrations, we only used samples with a loss on ignition <5 wt.% yielding a number of 56 out of a total of 83 samples. As an exception, we further consider the samples MSM82-80-DR-1 and MSM82-65-DR-2 with a loss on ignition of 5.8 and 5.3 wt.%, respectively, since these samples
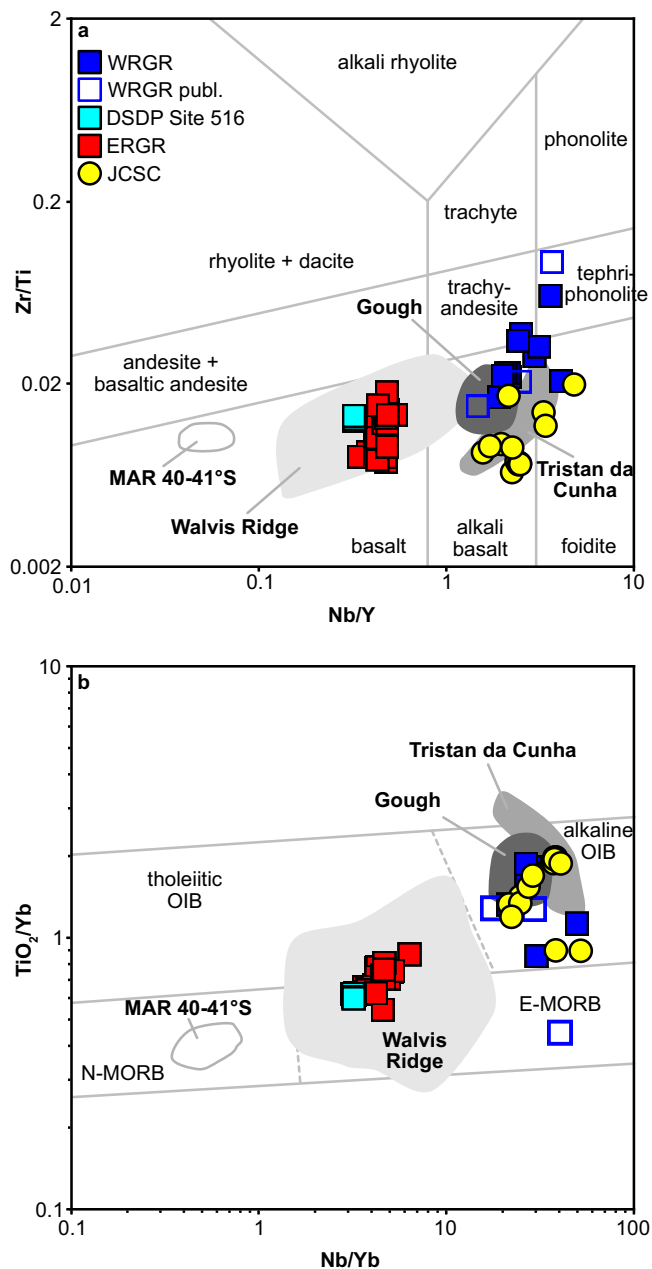
Fig. 2 Classification diagrams using fluid-immobile trace element ratios. **a** Nb/Y versus Zr/Ti discrimination diagram showing that the lavas of the Eastern Rio Grande Rise (ERGR) are relatively homogenous in composition and overlap with those from Deep Sea Drilling Program (DSDP) Site 516 and the Walvis Ridge[15,52]. In comparison, the alkaline samples of the Western Rio Grande Rise (WRGR) exhibit a wider geochemical variety and overlap with previously dredged alkaline rocks from the same area[18,20], the Jean Charcot Seamount Chain (JCSC) and those from the ocean islands of Tristan da Cunha and Gough[53–56]. **b** Nb/Yb and TiO₂/Yb discrimination diagram showing that the samples from the ERGR and those from the Walvis Ridge[15,52] and DSDP Site 516 follow a diagonal trend from the alkaline Ocean Island Basalt (OIB) field to the tholeiitic normal Mid-Ocean Ridge Basalt (N-MORB) field indicating plume–ridge interaction during their formation. In contrast, the alkaline lavas from the WRGR, the JCSC as well as those from present-day ocean islands plot with the alkaline OIB field. For comparison data from South Atlantic MORB[57] glass from 40 to 41°S are shown. Note, to minimize the effects of fractional crystallization processes, we only show samples with MgO ≥ 4 wt.%. Modified after Pearce[29,30].
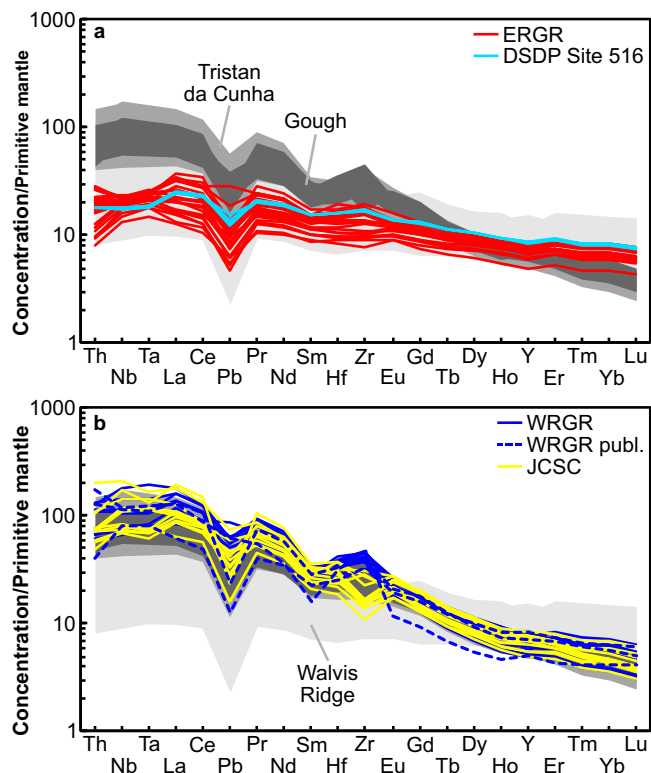

Fig. 3 Primitive mantle[58] normalized multielement variation diagrams showing geochemical differences between the tholeiitic lavas from the Rio Grande Rise and the alkaline lavas from the Rio Grande Rise and Jean Charcot Seamount Chain (JCSC). **a** The lavas samples from the Eastern Rio Grande Rise (ERGR) and Deep Sea Drilling Program (DSDP) Site 516 display trace element patterns similar to those of the Walvis Ridge[15,52]. **b** The lava samples from the Western Rio Grande Rise (WRGR) and JCSC exhibit trace element patterns similar to those of Tristan da Cunha and Gough. Note samples with MgO concentrations of <2 wt.% MgO are not shown.

macroscopically appear relatively fresh and are the least altered from the respective seamounts.

Seawater alteration has an influence on the concentration of fluid-mobile elements, such as K and other Large Ion Lithophile Elements in submarine volcanic rocks[28]. Thus, we focused our interpretation on fluid-immobile elements (e.g., Ti, Y, Zr, Nb, Hf, Th and rare earth elements), which are assumed to be resistant to seawater alteration[28]. We used classification diagrams applying fluid-immobile elements to distinguish between different rock types and oceanic settings. The Nb/Y vs. Zr/Ti discrimination diagram[29] reveals that our samples from the ERGR and WRGR are geochemically distinct (Fig. 2a), which is also observed in the Total-alkalis versus SiO₂ diagram (Supplementary Fig. 1). The lavas from the WRGR show highly variable compositions ranging from alkali basalt to trachyandesites, tephriphonolite and foidite similar to intraplate lavas from Tristan da Cunha and Gough (Fig. 2a). The alkaline rocks from the WRGR overlap in composition with those from the JCSC and previously dredged ~46 Ma old[16] alkaline volcanic rocks from the WRGR (Fig. 2a). In contrast, lavas from the ERGR are tholeiitic basalts and overlap with those from DSDP Site 516 and the Walvis Ridge (Fig. 2a). The lavas of the Walvis Ridge, ERGR and DSDP Site 516 show E-MORB-like (enriched Mid-Ocean Ridge Basalt) compositions and follow a diagonal trend from the OIB (Ocean Island Basalt) to the N-MORB (normal MORB) fields (Fig. 2b). In comparison, the new, as well as the published alkaline samples from the WRGR
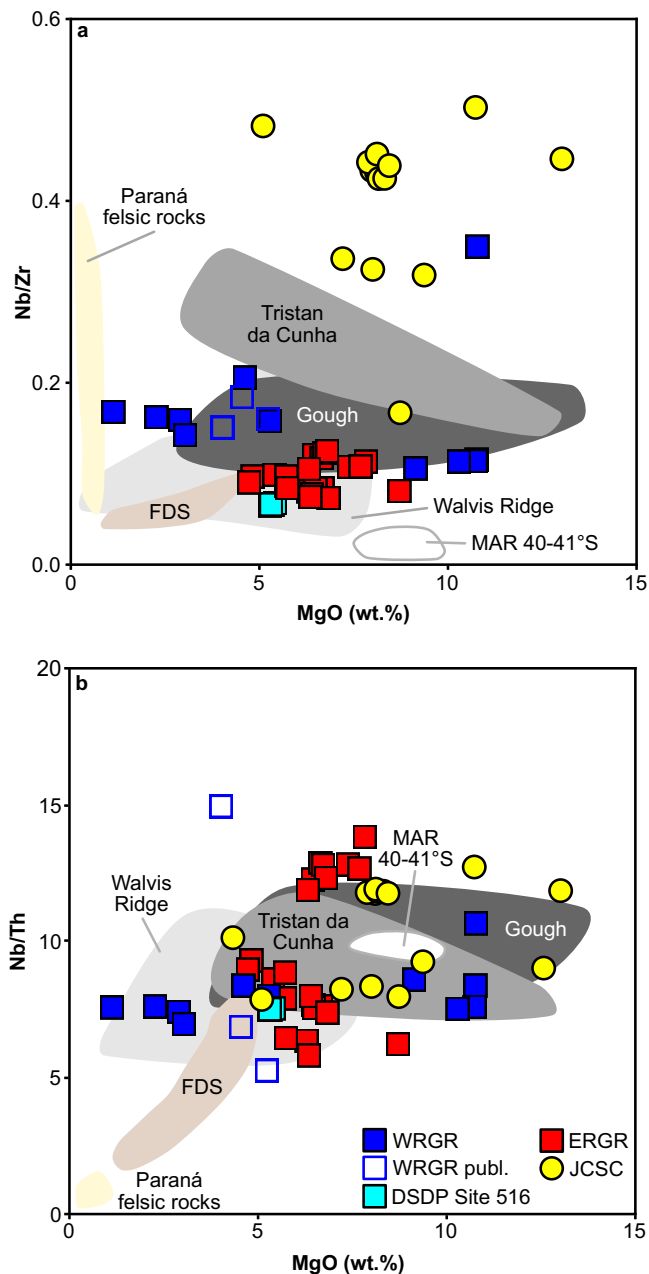
Fig. 4 Major and trace element ratios showing that the lavas of the Rio Grande Rise exhibit no clear geochemical indications for assimilation with continental crust. Major and trace element variations of **a** MgO versus Nb/Zr and **b** MgO versus Nb/Th are shown. For comparison lava flows from the Walvis Ridge[15,52] and the ocean islands of Tristan da Cunha and Gough[53–56] are shown. Further, we considered geochemical compositions of previously dredged samples from the Western Rio Grande Rise (WRGR)[18,20], glasses from South Atlantic Mid-Ocean Ridge Basalt (MORB)[57] and crustally contaminated lavas from the Florianópolis Dyke Swarm[36] (FDS) for comparison. The field of the Paraná felsic rocks include the Paulo Lopes Granites and Garopaba Granodiorites[35].

and JCSC, possess a OIB signature and overlap with lavas of Tristan da Cunha and Gough (Fig. 2b). Because some of the element ratios used for this classification diagram[30] are affected by fractional crystallization processes (particularly TiO_2), only samples with MgO contents ≥4 wt.% are shown.

In terms of a larger range of incompatible element compositions the new as well as the published alkaline WRGR samples

have distinct geochemical patterns from the Walvis Ridge, ERGR and DSDP Site 516 lavas, but are similar to those from the Tristan da Cunha, Gough, and JCSC (Fig. 3). The alkaline WRGR, Tristan da Cunha, Gough and JCSC lavas are enriched in light rare earth elements (LREE) and high field strength elements (e.g. Nb, Ta) as well as depleted in heavy rare earth elements (HREE) compared to the ERGR, DSDP Site 516 and Walvis Ridge lavas (Fig. 3).

Volcanic rocks from the ERGR have a relatively narrow compositional range of Nb/Zr at given MgO comparable to lavas from the Walvis Ridge and DSDP Site 516 (Fig. 4a). The alkaline lavas from the WRGR partly overlap with the lavas of the ERGR, but extend to higher ratios similar to samples from Gough (Fig. 4a). The JCSC is characterized by highly variable but elevated ratios of Nb/Zr (Fig. 4a). The lavas from DSDP Site 516, the alkaline lavas from the WRGR and the JCSC have variable ratios of Nb/Th between 6 and 14 similar to Tristan da Cunha, Gough and Walvis Ridge lavas. Importantly, the RGR lavas do not show decreasing trends of Nb/Zr and Nb/Th with decreasing MgO (Fig. 4b), indicating that fractional crystallization processes have not substantially affected these element ratios. In comparison, the ERGR exhibit variable ratios of Nb/Th at a given MgO with those having the highest ratios (~13) were sampled in close proximity (dredge sites MSM82-DR-6 and MSM82-DR-7) (Fig. 4b).

Bivariate plots of fluid-immobile incompatible element ratios show geochemical similarities between lavas from the ERGR, DSDP Site 516 and Walvis Ridge (Fig. 5). Rocks from the ERGR and Walvis Ridge overlap, whereas the alkaline lavas from the WRGR and JCSC resemble those from Tristan da Cunha and Gough (Fig. 5).

Discussion
Although the RGR is considered as a coherent Large Igneous Province, it was previously suggested that the eastern and western parts have distinct morphologies and geological histories[31]. To the best of our knowledge the ERGR had previously not been sampled, and the only information about the age and geochemical evolution of the WRGR were available from the 80 to 87 Ma[16] tholeiitic volcanic rocks at DSDP Site 516[12–14] and alkaline volcanic rocks from one dredge site along the CdSR with an age of ~46 Ma[16]. Plate tectonic modelling suggests that during the emplacement of the tholeiitic DSDP Site 516 lavas the WRGR and Walvis Ridge were formed together at a plume-influenced spreading centre[9,32]. Our trace element data for volcanic rocks from DSDP Site 516 support this model showing geochemical compositions similar to those from the Walvis Ridge for this time period, and intermediate between southern Mid-Atlantic Ridge MORB and alkalic lavas from Tristan da Cunha and Gough (Fig. 2b). In contrast, our new dredged samples from the WRGR have incompatible trace element-enriched geochemical signatures similar to the published alkaline WRGR samples as well as to those from Tristan da Cunha, Gough, and the JCSC (Figs. 2–5). The new and published alkaline WRGR lavas resemble each other geochemically (Figs. 2–5) and were both dredged from the crests of the CdSR, so that we infer a similar age of ~46 Ma for our new samples. The WRGR is therefore heterogeneous in both age and geochemical compositions.

Besides sampling the WRGR, we were also able to obtain volcanic rocks from the southernmost part of the N-S trending ERGR and provide here extensive geochemical data from this area (Fig. 1b). The ERGR is believed to have formed between 83 and 70 Ma[16,33] either along a southward propagating, plume-fed spreading axis[9], or as an eastern extension of the WRGR due to decreasing effects of the Tristan-Gough mantle plume[33].
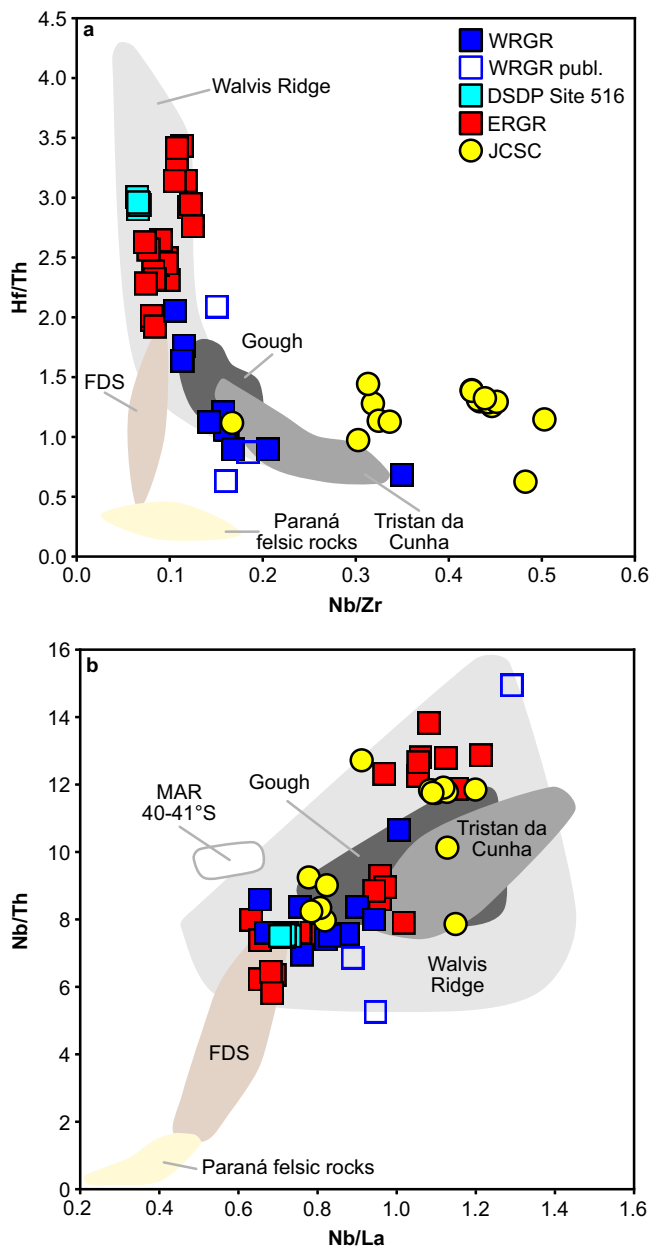
Fig. 5 Trace element ratios showing geochemical differences between the Eastern Rio Grande Rise (ERGR) and Western Rio Grande Rise (WRGR). Trace element variations of **a** Nb/Zr versus Hf/Th, and **b** Nb/La versus Nb/Th are shown. For comparison lava flows from the Walvis Ridge[15,52], and the ocean islands of Tristan da Cunha and Gough[53–56] are shown. Further, we considered geochemical compositions of previously dredged samples from the WRGR[18,20], glasses from South Atlantic Mid-Ocean Ridge Basalt (MORB)[57] and crustally contaminated lavas from the Florianopólis Dyke Swarm[36] (FDS) for comparison. The field of the Paraná felsic rocks include the Paulo Lopes Granites and Garopaba Granodiorites[35].

Our samples from the ERGR are incompatible trace element-enriched tholeiites and display similar geochemical characteristics to lavas from DSDP Site 516 and the Walvis Ridge (Figs. 2–5) possibly indicating a similar formation.

In contrast to the exclusively magmatic formation models, some studies suggest that the RGR is a microcontinent embedded in plume-influenced oceanic crust and covered by flood basalts[25,26] comparable to structures in the Indian and North Atlantic Oceans[3,34]. In particular the negative Bouguer anomaly

observed at the WRGR is interpreted as an indicator of continental crust[25,26], but other studies state that gravity inversion alone is inconclusive on the composition and origin of the RGR crust[17,21]. A recent study shows that the potential presence of of a microcontinent is only one of many explanations for the negative Bouguer anomaly observed at the RGR[21]. However, dredging at several locations on top of the WRGR recovered partly rounded boulders of gabbroic, granitic, and metamorphic rocks with thin Mn oxide coating[25]. Zircon U-Pb ages for these samples range from 480 to 2200 Ma which possibly indicates an origin from the Gondwana continent[25]. In contrast, our sampling of the slopes of the rifted western and eastern parts of the RGR even at water depths of >3000 m recovered exclusively angular volcanic rocks ranging from mafic to intermediate compositions (Fig. 2a). These rocks were dredged from different depths and locations, and in combination with the lavas from DSDP Site 516 (Fig. 1), we believe they provide a representative overview of the submarine plateau.

If the lavas exposed in the area of the RGR are underlain by fragments of continental crust, we would expect that at least some of them show geochemical indications for crustal assimilation. In general, the predominantly felsic continental crust differs geochemically from mafic mantle-derived magmas. For example, the Paulo Lopes Granites and Garopaba Granodiorites[35] exposed in the southern part of the Parana continental flood basalt province in Brazil (Fig. 1a) have relatively low ratios of Nb/La, Nb/Th, Hf/Th and Nb/Zr compared to mafic uncontaminated volcanic rocks from the Walvis Ridge (Figs. 4 and 5). Lavas from the Florianópolis Dyke Swarm (Fig. 1a) were contaminated by up to 15% with the Paulo Lopes Granites and Garopaba Granodiorites[36] and plot in between the fields of these continental rocks and the Walvis Ridge (Figs. 4 and 5). The crustally contaminated lavas also partly overlap with some rocks of the WRGR and ERGR (Figs. 4 and 5), but if the latter were affected by crustal assimilation, these rocks should display a positive correlation between MgO and Nb/Th similar to the Florianópolis Dyke Swarm lavas (Fig. 4b). Nb and Th are neither fractionated by crystallization processes nor are these elements mobile during seawater alteration[28]. Typically, assimilation of continental material during stagnation and fractional crystallization in the crust would cause decreasing Nb/Th with decreasing MgO in a lava suite. In contrast, the DSDP Site 516 and alkaline WRGR lavas display relatively constant ratios of Nb/Th with decreasing MgO (Fig. 4b) which indicates extensive assimilation-fractional crystallization processes in the area of the WRGR is unlikely. Similarly, the high Nb/Th and Hf/Th of the lavas from the ERGR resemble volcanic rocks from the Walvis Ridge but are generally unlike the contaminated lavas of the Florianopolis Dyke Swarm (Fig. 5). Geochemical variability occurs in the ERGR samples at MgO > 5 wt.% with two groups with different Nb/Th ratios that probably reflect a heterogenous mantle source rather than crustal assimilation (Fig. 4). Thus, we find no evidence that the RGR lavas experienced crustal contamination and therefore suggest that the plateau is dominantly volcanic in origin. These findings are consistent with recent wide-angle seismic data gathered from across the RGR, which show a typical velocity-depth distribution for submarine large igneous provinces[37]. The previously dredged granitic rocks from the summit of the RGR are likely to represent ice-rafted material rather than in situ samples from the continental crust.

Because the lavas of the RGR appear to be unaffected by crustal contamination, we use the rare earth element compositions to estimate the melting conditions of both the tholeiitic and alkaline magmatic phases of the RGR. We applied the REEBOX Pro (v.1) melting algorithm from Brown and Lesher[38], which calculates the trace element compositions of pooled melts over a range of

pressures between the mantle solidus and the base of the rigid lithosphere. Due to the retention of the HREE relative to the middle rare earth element (MREE) in residual garnet, ratios of these elements reflect changes in the depth of melting[39,40]. The latter depends on the composition and temperature of the upwelling mantle which defines the depth of solidus intersection and thus the beginning of partial melting. The degree of melting is controlled by the length of the melting column which is limited by the thickness of the overlying lithosphere, and also increases with increasing mantle temperature. Since the MREE are less incompatible than the LREE in mantle minerals, higher ratios of LREE/MREE reflect a lower degree of melting[39,40]. Subsequent fractional crystallization has little effect on the ratios of rare earth elements or other highly incompatible elements used in the modelling.

Modelling of decompression melting requires assumptions about the mantle source. From published isotope data it is evident that the source regions associated with the South Atlantic volcanism and more specific with the Tristan-Gough mantle plume are heterogeneous in composition[15]. In the case of the RGR, isotope data for the ~87 to ~80 Ma DSDP Site 516 tholeiites and the ~46 Ma alkaline WRGR lavas reveal source heterogeneity during the formation of the submarine plateau[15,20]. Our new alkaline WRGR lavas display higher ratios of Nb/Zr at a given MgO compared to the DSDP Site 516 tholeiites and the ERGR indicating a more enriched mantle source for the former (Fig. 4a). Since the DSDP Site 516 and ERGR lavas display E-MORB-like geochemical characteristics (Fig. 2b), we define a source consisting of 80% depleted MORB mantle[41] and 20% primitive mantle[42] possibly reflecting the interaction of depleted upper mantle with enriched plume material. In contrast, the alkaline WRGR lavas overlap with OIB-like geochemical compositions, which is why we assume a more enriched source consisting of 70% primitive mantle[42] and 30% depleted MORB mantle[41].

To estimate the degree and depths of melting during the emplacement of the DSDP Site 516, ERGR and WRGR lavas, we modelled partial melting for different mantle potential temperatures (T_P) (Fig. 6). The latter range from 1380 to 1480 °C (20 °C steps), and the changes in the trace element compositions during progressive decompression melting are illustrated by black solid lines in Fig. 6. The degrees of melting is indicated in 1% steps and shown by red dashed lines (Fig. 6). The pressure estimates within our model range from 2.0 to 3.2 GPa, shown by the black dashed lines representing 0.1 GPa steps (Fig. 6). Since no pre-existing lithosphere was assumed in the modelling, for each T_P ratios of $(La/Sm)_N$ and $(Dy/Yb)_N$ progressively decrease with increasing degrees of melting and decreasing pressure (Fig. 6).

The tholeiitic DSDP Site 516 and ERGR lavas with MgO contents ≥4 wt.% indicates moderate degrees of partial melting between 2% and 5% coupled with low pressures <2.7 GPa which is consistent with an origin at or close to a plume-influenced spreading centre (Fig. 6a). The lavas can be modelled with a T_P between ~1400 and 1440 °C (Fig. 6a) which is comparable to recent temperature estimates for the Tristan da Cunha hotspot ranging from 1410 to 1430 °C[43]. The modelled T_P yield crustal thicknesses between ~15 and ~19 km which are similar to the current crustal thickness estimates in the area of the ERGR (~15 to ~17 km)[17,37]. In comparison, the alkaline basalts recovered from the WRGR apparently formed by low degrees of partial melting between 0.5 and 2% at pressures >2.9 GPa (Fig. 6b) possibly reflecting partial melting beneath a plate distant from the spreading axis. The majority of lavas can be modelled with T_P ranging between 1420 and 1440 °C (Fig. 6b) yielding crustal thicknesses between ~21 and ~24 km which are somewhat
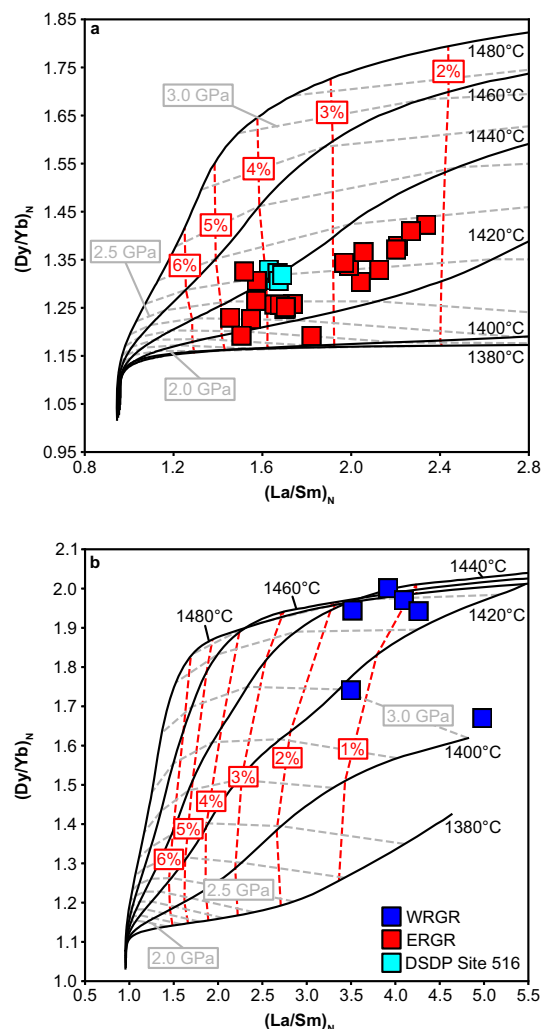

Fig. 6 Trace element-based melt model results showing partial melting over a range of different pressures and mantle potential temperatures. The melt model algorithm was taken from Brown and Lesher[38]. The mantle potential temperatures ranging from 1380 to 1480 °C (20 °C steps), whereby the changes in the trace element compositions during each decompression step are illustrated by black solid lines. The degrees of melting are indicated in 1% steps and shown by red dashed lines. The pressure estimates range from 3.2 to 1.5 GPa, whereby 0.1 GPa steps are given by grey dashed lines. For each mantle potential temperature, ratios of $(La/Sm)_N$ and $(Dy/Yb)_N$ temporally decline reflecting increasing degrees of melting with decreasing pressures. **a** The lavas of Deep Sea Drilling Program (DSDP) Site 516 show a degree of melt of ~4 %, a mantle potential temperature of 1440 °C and model pressures of ~2.6 GPa. In comparison, the lavas of the Eastern Rio Grande Rise (ERGR) show degrees of melting from ~2 to ~5%, mantle potential temperatures ranging from 1400 to 1450 °C and model pressures between ~2.2 and 2.7 GPa. For melt modeling we assumed a mantle source consisting of 80 % depleted MORB mantle[41] and 20 % primitive mantle[42]. **b** The lavas of the Western Rio Grande Rise (WRGR) show degrees of melting from ~0.5 to ~2 %, mantle potential temperatures ranging from 1420 to 1440 °C and model pressures between ~3.0 and 3.2 GPa. For melt modeling we assumed a mantle source consisting of 30% depleted MORB mantle[41] and 70% primitive mantle[42]. Note, one sample plot outside the melting grid and cannot be modelled by the assumed melting parameters. To minimize the effects of fractional crystallization processes, we only show samples with MgO ≥ 4 wt.%. Trace element ratios are normalized to chondrite[59].

less than recent crustal thickness estimates in the area of the WRGR (~25 km)[17]. For both the ERGR and WRGR, an effect by a deep mantle plume is supported by the fact that both areas have a considerably thicker crust than average oceanic crust (~7 ± 1 km)[44] and the potential temperatures of the mantle required are higher than average asthenosphere mantle temperature (~1330 °C).

A shift from a voluminous tholeiitic shield stage to late-stage alkaline rocks is a common feature of mantle plume-related ocean intraplate volcanism[45]. However, late-stage volcanism usually occurs a few million years after the formation of the main tholeiitic volcanic edifices, whereas the change from the tholeiitic stage to the alkaline melts of the RGR occurred over tens of millions of years. Recent ^{40}Ar-^{39}Ar age dating of WRGR lavas suggest ages of 87–80 Ma for the tholeiites of DSDP Site 516, whereas the age-dated alkaline WRGR samples yield an age of 46 Ma[16]. These authors suggest that the early tholeiitic stage occurred when the RGR formed together with the Walvis Ridge close to a spreading axis, which is consistent with our melting model, indicating moderate degrees of melting at shallow depths (Fig. 6a). The Walvis Ridge was affected by a widespread volcanic event 20–40 Ma after its formation[20], but it is unlikely that the same processes were responsible for the alkaline stage of the WRGR, because the two plateaus were separated at that time. In accordance with this, the ~46 Ma alkaline WRGR samples exhibit lower $^{207}Pb/^{204}Pb$ and $^{208}Pb/^{204}Pb$ ratios for a given $^{206}Pb/^{204}Pb$ isotope ratio compared to the late-stage samples from the Walvis Ridge indicating derivation from different mantle sources[20].

The geochemical similarity of the alkaline WRGR lavas to some of the JCSC lavas may indicate that the former is related to volcanic activity forming this seamount chain at the northwestern prolongation of the CdSR (Fig. 1). The JCSC lavas resemble those from oceanic seamount chains, for example, those from Tristan da Cunha and Gough (Figs. 2–5). The deep melting of an enriched mantle source suggested by the major and incompatible trace element compositions (Figs. 2–5) implies low degrees of partial melting beneath a thick lithosphere. The northwestern section of the JCSC lies on the prolongation of the CdSR (Fig. 1), which is believed to represent an Eocene rift zone[21,26]. Tectonic models suggest lithospheric rifting[21,26] that typically causes thinning of the lithosphere and deep partial melting of the asthenosphere, thereby initiating the alkaline WRGR and JCSC volcanism. Although the lavas of the JCSC generally display similar geochemical characteristics to those from the WRGR (Figs. 2–5), some incompatible element ratios indicate that the lavas of both locations were fed from different mantle regions (Fig. 5). For example, the alkaline WRGR and some of the JCSC lavas overlap with those from Gough Island in terms of Hf/Th, Nb/La, Nb/Th and Nb/Zr, but most of the JCSC samples have higher ratios of Nb/La and Nb/Zr, to some extent resembling Tristan da Cunha basalts (Fig. 5). Thus, we suggest that the late-stage volcanism of the WRGR on the flanks of the CdSR was formed by Eocene rifting of the thick lithosphere of the RGR which may have also caused magma generation of the JCSC (Fig. 7). However, the WRGR and JCSC lavas were probably derived from compositionally different sources, indicating small-scale mantle heterogeneity beneath the western South Atlantic Ocean. We note that volcanic rocks with ages of ~51 Ma[46] are also known from Cabo Frio at the coast of Brazil (Fig. 1a), and previous studies suggested faults crosscutting the continental and oceanic lithosphere[47–49]. In this case, the formation of the alkaline WRGR-JCSC volcanism may therefore have been comparable to that of the recent volcanic belt of the Cameroon Line crossing from continental into oceanic lithosphere[50,51]. The RGR is therefore a complex volcanic plateau formed over at least several tens of millions of years in response to plume–ridge interaction and lithospheric rifting.
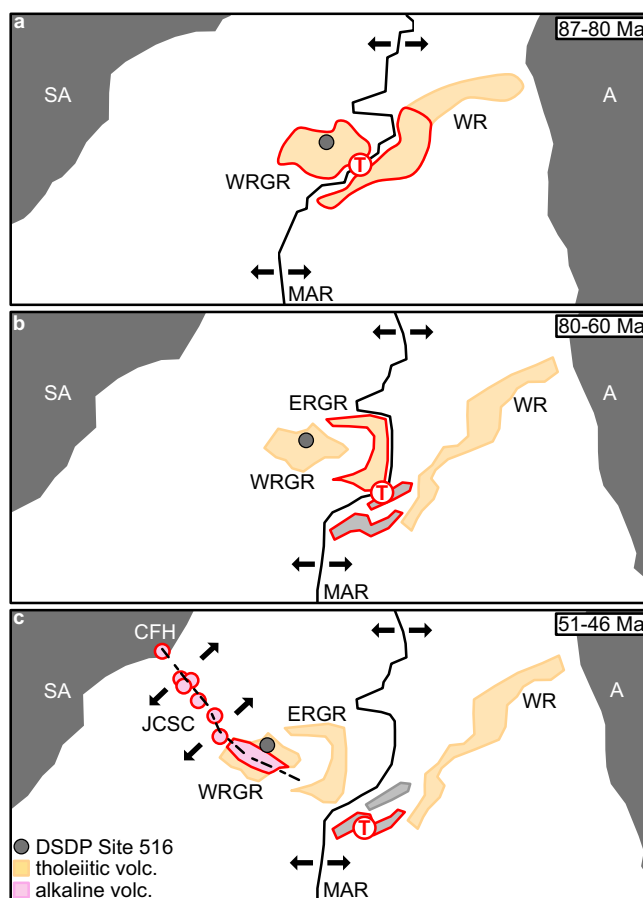

Fig. 7 Schematic sketch illustrating the geochemical and tectonic evolution of the Rio Grande Rise and Jean Charcot Seamount Chain (JCSC). a 87–80 Ma ago, the interaction of the Tristan-Gough mantle plume (red circled T) with the Mid-Atlantic Ridge (MAR) caused the formation of the western Rio Grande Rise (WRGR) and Walvis Ridge (WR). During this stage the tholeiitic Deep Sea Drilling Program (DSDP) Site 516 lavas were formed by high degrees of shallow melting of slightly enriched upper mantle material. **b** Between 80 and 60 Ma seafloor spreading separated the WRGR and WR and the tholeiitic eastern Rio Grande Rise (ERGR) lavas were formed due to plume–ridge interaction similar to those from DSDP Site 516. **c** Between 51 and 46 Ma, die formation of the Cruzeiro do Sul Rift (black dashed line) caused lithospheric rifting and possibly initiated the alkaline magmatism at the WRGR and Cabo Frio High as well as the formation of the JCSC. The Tristan-Gough mantle plume was situated beneath the African Plate during this time. The yellowish areas were formed by tholeiitic volcanism, the pink areas by alkaline volcanism. Areas outlined in red indicate active volcanism at this time. Black arrows indicate seafloor spreading at the MAR and lithospheric rifting during the formation of the Cruzeiro do Sul Rift. Abbreviations are as follows: SA South America, A Africa.

Methods
Sampling. The samples considered in this study were collected during research cruise MSM-82 with RV Maria S. Merian in March/April 2019. In total 47 volcanic rocks were sampled from submarine structures with steep flanks and little sediment cover from both the ERGR (seven sites) and the WRGR (six sites). Furthermore, 31 samples were taken from six submarine volcanoes of the JCSC (Fig. 1). The rocks were obtained by dredging from water depths ranging from 915 m to 5266 m below sea level.

Sample preparation. Selected samples were cut on board into blocks with a rock saw for both thin-section preparation and geochemical analyses. For the latter, the altered rims and manganese crusts were removed and only the fresh-looking interiors of the rocks were retained. On land, the pieces were cleaned in an ultrasonic bath with deionized water and dried at 60 °C for 12 h. Subsequently the

blocks were coarsely crushed using a hydraulic press and unaltered fragments were pulverized in an agate mill. Prior to further geochemical analyses, the powders were dried at 105 °C for 12 h. In addition, five drill core samples from DSDP Site 516 were obtained from the IODP Bremen core repository. These samples were prepared using the same method as described above.

Major and trace element analyses. For major and selected trace element measurements whole-rock powders were mixed with lithium tetraborate, fused to glass beads and analyzed using a Spectro XEPOS He X-ray fluorescence spectrometer at the GeoZentrum Nordbayern, Friedrich-Alexander-Universität Erlangen-Nürnberg. Repeated measurements ($n = 5$) of the international rock standard BE-N yielded a precision better than 1.2% and an accuracy better than 4.2%, except for P_2O_5 (12.8%).

Trace element analyses were carried out using a Thermo X-Series2 quadrupole ICP-MS at the GeoZentrum Nordbayern in Erlangen. Approximately 50 mg of sample powder was accurately weighed into a Teflon beaker, wetted with a few drops of 15 M HNO_3, before adding 2 ml 12 M HF. Samples were digested in the sealed beakers for 24 hours at 80 °C. Three drops of concentrated perchloric acid were then added, and the solution evaporated to near dryness at 125 °C. The residue was treated three times with 2 ml 15 M HNO_3 and evaporated at 145 °C to fume off the perchloric acid. Samples were then re-dissolved in a solution of 4 ml 15 M HNO_3, 5 ml H_2O and 1 drop 12 M HF in sealed beakers overnight, allowed to cool, before transferring quantitatively to HDPE bottles and diluting to 200 g with H_2O. Sample solutions were mixed online with a Be-In-Rh-Bi internal standard solution, and introduced into the plasma via a Cetac Aridus II desolvating nebuliser. The ICP-MS was tuned using a mixed Li-Ce-In-U solution in order to obtain maximum sensitivity (typically 40,000 cps/ppb for ^{238}U) and low oxide production (Ce/CeO > 5000). Multiple analyses of the BHVO-2 Hawaiian rock standard give accuracy and precision better than 5% and 3%, respectively.

Trace element modelling. Trace element modelling was carried out using the REEBOX Pro (v.1) melting algorithm from Brown and Lesher[38]. The model calculates the trace element compositions of pooled melts that were formed over a range of pressures by using the latest melting reactions and mineral/melt partitions coefficients. For this, the region between the bottom (mantle solidus) and the top (base of the rigid lithosphere) of the melting columns are subdivided into several decompression steps, in each of which small quantities of melt are formed. The trace element concentrations of these instantaneous melts are calculated by using non-modal batch melting, while those of the residue is obtained by using mass balance[38]. The remaining mantle of the previous decompression step is assumed to ascend to slightly lower pressures and partially melts again simulating progressive depletion of the upwelling source. The instantaneous melts formed along individual melting columns are accumulated at the top of each melting column. Then these accumulated melts are aggregated from the base to the top of the melting zone forming the pooled melt compositions. Since it is believed that the tholeiitic lavas of the WRGR were formed at a plume-influenced spreading center, we modelled an active upwelling scenario by using suitable mixing functions describing how instantaneous melts are aggregated within the melting zone[38]. Independently from the mixing functions, the transition from the garnet to spinel stability field has an influence on the geochemical compositions of the pooled melts. For a pyrolite peridotite (enriched mantle) the REEBOX Pro application assumes that garnet is stable at pressures above 2.7 GPa, whereas spinel exists below 3 GPa, respectively. Hence, both phases are stable in a 0.3 GPa transition field[38].

Data availability
Major and trace element data produced during this study are provided in Supplementary Data 1 and are openly available in the EarthChem database at https://doi.org/10.26022/IEDA/112205.

Code availability
The REEBOX PRO (v.1) application utilized in this study can be downloaded at http://geo.au.dk/forskning/forskningscentre/earth-system-petrology/reebox-pro/.

References
1. Wilson, J. T. A possible origin of the Hawaiian Islands. *Can. J. Phys.* **41**, 863–870 (1963).
2. Gladczenko, T. P., Coffin, M. F. & Eldholm, O. Crustal structure of the Ontong Java Plateau: modeling of new gravity and existing seismic data. *J. Geophys. Res. Solid Earth* **102**, 22711–22729 (1997).
3. Gudlaugsson, S. T., Gunnarsson, K., Sand, M. & Skogseid, J. Tectonic and volcanic events at the Jan Mayen Ridge microcontinent. *Geol. Soc. Lond. Special Publ.* **39**, 85–93 (1988).
4. Dickin, A. P., Fallick, A. E., Halliday, A. N., Macintyre, R. M. & Stephens, W. E. An isotopic and geochronological investigation of the younger igneous rocks of the Seychelles microcontinent. *Earth Planet. Sci. Lett.* **81**, 46–56 (1986).
5. Borissova, I., Coffin, M. F., Charvis, P. & Operto, S. Structure and development of a microcontinent: Elan Bank in the southern Indian Ocean. *Geochem. Geophys. Geosyst.* **4**, 1071 (2003).
6. Wilson, J. T. Hypothesis of earth's behaviour. *Nature* **198**, 925–929 (1963).
7. Wilson, J. T. Submarine fracture zones, aseismic ridges and the International Council of Scientific Unions line: proposed western margin of the east Pacific ridge. *Nature* **207**, 907–911 (1965).
8. Morgan, W. J. Convection plumes in the lower mantle. *Nature* **230**, 42–43 (1971).
9. O'Connor, J. M. & Duncan, R. A. Evolution of the Walvis Ridge-Rio Grande Rise hot spot system: Implications for African and South American plate motions over plumes. *J. Geophys. Res. Solid Earth* **95**, 17475–17502 (1990).
10. O'Connor, J. M. & Jokat, W. Age distribution of Ocean Drill sites across the Central Walvis Ridge indicates plate boundary control of plume volcanism in the South Atlantic. *Earth Planet. Sci. Lett.* **424**, 179–190 (2015).
11. Humphris, S. E. & Thompson, G. Geochemistry of rare earth elements in basalts from the Walvis Ridge: implications for its origin and evolution. *Earth Planet. Sci. Lett.* **66**, 223–242 (1983).
12. Musset, A. E. & Baker, P. F. 40Ar/39Ar age spectra of basalts. DSDP project Site 516. *Initial Rep. Deep Sea Drill. Project* **72**, 467–480 (1983).
13. Weaver, B. L., Marsh, N. G. & Tarney, J. Trace-element geochemistry of basaltic rocks recovered at site-516, RIO-grande rise, deep-sea drilling project LEG-72. *Initial Rep. Deep Sea Drill. Project* **72**, 451–456 (1983).
14. Thompson, G., Humphris, S. & Schilling, J. G. Petrology and geochemistry of basaltic rocks from rio-grande rise, south-atlantic-deep-sea drilling project LEG-72, HOLE-516F. *Initial Rep. Deep Sea Drill. Project* **72**, 457–466 (1983).
15. Hoernle, K. et al. How and when plume zonation appeared during the 132 Myr evolution of the Tristan hotspot. *Nat. Commun.* **6**, 1–10 (2015).
16. Rohde, J. K., van den Bogaard, P., Hoernle, K., Hauff, F. & Werner, R. Evidence for an age progression along the Tristan-Gough volcanic track from new 40Ar/39Ar ages on phenocryst phases. *Tectonophysics* **604**, 60–71 (2013).
17. Graça, M. C., Kusznir, N. & Stanton, N. S. G. Crustal thickness mapping of the central South Atlantic and the geodynamic development of the Rio Grande Rise and Walvis Ridge. *Marine Petroleum Geol.* **101**, 230–242 (2019).
18. Fodor, R. V., Husler, J. W. & Kumar, N. Petrology of volcanic rocks from an aseismic rise: implications for the origin of the Rio Grande Rise, South Atlantic Ocean. *Earth Planet. Sci. Lett.* **35**, 225–233 (1977).
19. Bryan, W. B. & Duncan, R. A. Age and provenance of clastic horizons from HOLE-516F. *Initial Rep. Deep Sea Drill. Project* **72**, 475–477 (1983).
20. Homrighausen, S. et al. Unexpected HIMU-type late-stage volcanism on the Walvis Ridge. *Earth Planet. Sci. Lett.* **492**, 251–263 (2018).
21. Mohriak, W. U., Nóbrega, M., Odegard, M. E., Gomes, B. S. & Dickson, W. G. Geological and geophysical interpretation of the Rio Grande Rise, south-eastern Brazilian margin: extensional tectonics and rifting of continental and oceanic crusts. *Petroleum Geosci.* **16**, 231–245 (2010).
22. De Souza, K. G. et al. in *3rd International Congress of the Brazilian Geophysical Society*. cp-324-00258 (European Association of Geoscientists & Engineers, 1993).
23. Pinheiro Praxedes, A. G., de Castro, D. L., Torres, L. C., Gambôa, L. A. P. & Hackspacher, P. C. New insights of the tectonic and sedimentary evolution of the Rio Grande Rise, South Atlantic Ocean. *Marine Petroleum Geol.* **110**, 335–346 (2019).
24. Sandwell, D. T. & Smith, W. H. F. Global marine gravity from retracked Geosat and ERS-1 altimetry: ridge segmentation versus spreading rate. *J. Geophys. Res. Solid Earth* **114**, B01411 (2009).
25. Santos, R. V. et al. Dating Gondwanan continental crust at the Rio Grande Rise, South Atlantic. *Terra Nova* **31**, 424–429 (2019).
26. Ussami, N., Chaves, C. A. M., Marques, L. S. & Ernesto, M. Origin of the Rio Grande Rise–Walvis Ridge reviewed integrating palaeogeographic reconstruction, isotope geochemistry and flexural modelling. *Geol. Soc. Lond. Special Publ.* **369**, 129–146 (2013).
27. Barker, P. F. et al. SITE-516-RIO-GRANDE RISE. *Initial Rep. Deep Sea Drill. Project* **72**, 155–338 (1983).
28. Verma, S. P. Seawater alteration effects on 87Sr86Sr, K, Rb, Cs, Ba and Sr in oceanic igneous rocks. *Chem. Geol.* **34**, 81–89 (1981).
29. Pearce, J. A. A User's Guide to Basalt Discrimination Diagrams in *Trace Element Geochemistry of Volcanic Rocks: Applications for Massive Sulphide Exploration* (ed. Wyman, D.A.) **12**, 79–113 (Geological Association of Canada. Short Course Notes, 1996).
30. Pearce, J. A. Geochemical fingerprinting of oceanic basalts with applications to ophiolite classification and the search for Archean oceanic crust. *Lithos* **100**, 14–48 (2008).
31. Camboa, L. A. P. & Rabinowitz, P. D. The evolution of the Rio Grande Rise in the southwest Atlantic Ocean. *Marine Geol.* **58**, 35–58 (1984).
32. O'Connor, J. M. & Le Roex, A. P. South Atlantic hot spot-plume systems: 1. Distribution of volcanism in time and space. *Earth Planet. Sci. Lett.* **113**, 343–364 (1992).

33. Sager, W. W., Thoram, S., Engfer, D. W., Koppers, A. A. P. & Class, C. Late Cretaceous Ridge Reorganization, Microplate Formation, and the Evolution of the Rio Grande Rise–Walvis Ridge Hot Spot Twins, South Atlantic Ocean. *Geochem. Geophys. Geosyst.* **22**, e2020GC009390 (2021).

34. Torsvik, T. H. et al. A Precambrian microcontinent in the Indian Ocean. *Nat. Geosci.* **6**, 223–227 (2013).

35. Florisbal, L. M., de Fátima Bitencourt, M., Nardi, L. V. S. & Conceição, R. V. Early post-collisional granitic and coeval mafic magmatism of medium-to high-K tholeiitic affinity within the Neoproterozoic Southern Brazilian Shear Belt. *Precambr. Res.* **175**, 135–148 (2009).

36. Marques, L. S. et al. Elemental and Sr-Nd-Pb isotope geochemistry of the Florianópolis Dyke Swarm (Paraná Magmatic Province): crustal contamination and mantle source constraints. *J. Volcanol. Geothermal Res.* **355**, 149–164 (2018).

37. Altenbernd, T., Geissler, W. H., Jokat W. –*AGU Fall meeting*. https://agu.confex.com/agu/fm21/meetingapp.cgi/Paper/897483. (2021).

38. Brown, E. L. & Lesher, C. E. REEBOX PRO: A forward model simulating melting of thermally and lithologically variable upwelling mantle. *Geochem. Geophys. Geosyst.* **17**, 3929–3968 (2016).

39. Ellam, R. M. Lithospheric thickness as a control on basalt geochemistry. *Geology* **20**, 153–156 (1992).

40. Haase, K. M. & Devey, C. W. Geochemistry of lavas from the Ahu and Tupa volcanic fields, Easter Hotspot, southeast Pacific: implications for intraplate magma genesis near a spreading axis. *Earth Planet. Sci. Lett.* **137**, 129–143 (1996).

41. Workman, R. K. & Hart, S. R. Major and trace element composition of the depleted MORB mantle (DMM). *Earth Planet. Sci. Lett.* **231**, 53–72 (2005).

42. McDonough, W. F. & Sun, S.-S. The composition of the Earth. *Chem. Geol.* **120**, 223–253 (1995).

43. Bonadio, R. et al. Hot upper mantle beneath the Tristan da Cunha hotspot from probabilistic Rayleigh-wave inversion and petrological modeling. *Geochem. Geophys. Geosyst.* **19**, 1412–1428 (2018).

44. Bown, J. W. & White, R. S. Variation with spreading rate of oceanic crustal thickness and geochemistry. *Earth Planet. Sci. Lett.* **121**, 435–449 (1994).

45. Clague, D. A. & Dalrymple, G. B. The Hawaiian-Emperor volcanic chain. part I. Geologic evolution. *Volcanism Hawaii* **1**, 5–54 (1987).

46. Amaral, G., Bushee, J. C. U. G., Cordani, U. G., Kawashita, K. & Reynolds, J. H. Potassium-argon ages of alkaline rocks from southern Brazil. *Geochim. Cosmochim. Acta* **31**, 117–142 (1967).

47. Marsh, J. S. Relationships between transform directions and alkaline igneous rock lineaments in Africa and South America. *Earth Planet. Sci. Lett.* **18**, 317–323 (1973).

48. Riccomini, C., Velázquez, V. F. & Gomes, C. B. Tectonic controls of the Mesozoic and Cenozoic alkaline magmatism in central-southeastern Brazilian Platform. *Mesozoic to Cenozoic alkaline magmatism in the Brazilian Platform* **123**, 31–56 (2005).

49. Ferroni, F. R., Mello, C. L. & Destro, N. Tectonic control on the Cabo Frio anorogenic magmatic lineament, Southeastern Brazil. *J. South Am. Earth Sci.* **83**, 37–54 (2018).

50. Fitton, J. G. The Cameroon line, West Africa: a comparison between oceanic and continental alkaline volcanism. *Geol. Soc. Lond. Special Publ.* **30**, 273–291 (1987).

51. Déruelle, B., Ngounouno, I. & Demaiffe, D. The 'Cameroon Hot Line' (CHL): a unique example of active alkaline intraplate structure in both oceanic and continental lithospheres. *Comptes Rendus Geosci.* **339**, 589–600 (2007).

52. Salters, V. J. M. & Sachi-Kocher, A. An ancient metasomatic source for the Walvis Ridge basalts. *Chem. Geol.* **273**, 151–167 (2010).

53. Willbold, M. & Stracke, A. Trace element composition of mantle end-members: implications for recycling of oceanic and upper and lower continental crust. *Geochem. Geophys. Geosyst.* **7**, Q04004 (2006).

54. Salters, V. J. M., Mallick, S., Hart, S. R., Langmuir, C. E. & Stracke, A. Domains of depleted mantle: new evidence from hafnium and neodymium isotopes. *Geochem. Geophys. Geosyst.* **12**, Q08001 (2011).

55. Willbold, M. & Stracke, A. Formation of enriched mantle components by recycling of upper and lower continental crust. *Chem. Geol.* **276**, 188–197 (2010).

56. Weaver, B. L., Wood, D. A., Tarney, J. & Joron, J. L. Geochemistry of ocean island basalts from the south Atlantic: Ascension, Bouvet, St. Helena, Gough and Tristan da Cunha. *Geol. Soc. Lond. Special Publ.* **30**, 253–267 (1987).

57. Le Roux, P. J. et al. Mantle heterogeneity beneath the southern Mid-Atlantic Ridge: trace element evidence for contamination of ambient asthenospheric mantle. *Earth Planet. Sci. Lett.* **203**, 479–498 (2002).

58. Hofmann, A. W. Chemical differentiation of the Earth: the relationship between mantle, continental crust, and oceanic crust. *Earth Planet. Sci. Lett.* **90**, 297–314 (1988).

59. Sun, S. S. & McDonough, W. F. Chemical and isotopic systematics of oceanic basalts: implications for mantle composition and processes. *Geol. Soc. Lond. Special Publ.* **42**, 313–345 (1989).

Author contributions

P.A.H. was primary interpreter of the data and writer of the manuscript as well as was involved in sample collection and generating the major and trace element data. K.M.H. was involved in the interpretation of the data and writing of the manuscript. M.R. was involved in the interpretation of the data, writing of the manuscript and the generation of geochemical data. J.M.O'C. was involved in the interpretation of the data, writing of the manuscript and the sample collection. S.H. was involved in the interpretation of the data, writing of the manuscript and the sample collection. W.H.G. was involved in the interpretation of the data and writing of the manuscript. W.J. was involved in the interpretation of the data and writing of the manuscript.

Competing interests

The authors declare no competing interests.

Additional information

Supplementary information The online version contains supplementary material available at https://doi.org/10.1038/s43247-022-00349-1.

Correspondence and requests for materials should be addressed to Patrick A. Hoyer.

Peer review information *Communications Earth & Environment* thanks Chris Hawkesworth, Eduardo R. V. Rocha-Junior and the other, anonymous, reviewer(s) for their contribution to the peer review of this work. Primary Handling Editor: Joe Aslin

Reprints and permission information is available at http://www.nature.com/reprints

Publisher's note Springer Nature remains neutral with regard to jurisdictional claims in published maps and institutional affiliations.